

Final Report

NASA Research Grant NAG 9-768

Final
NAG 9-768
Final
93052

October 1, 1996

The basic research into space debris supported by NASA Research Grant NAG 9-768 is summarized in the two reports:

“ODERACS 2 White Spheres Optical Calibration Report”
and
“Polarization Signals of Common Spacecraft Materials.”

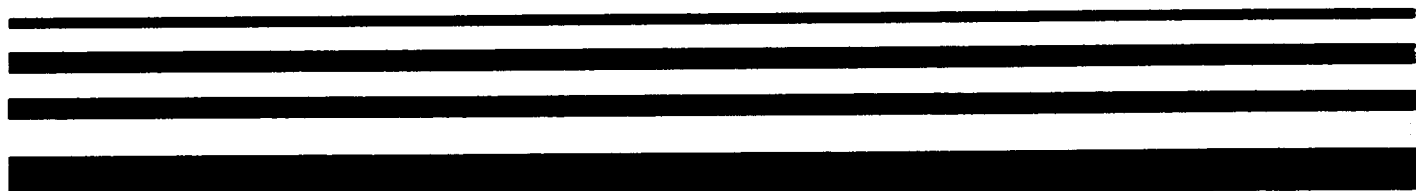
The reports were furnished previously as specified in the grant, and are attached as part of this final report. This grant is complete as of September 30, 1996. All funds have been expended. No government-owned property was obtained through this grant. No patents or licenses were generated by this grant.

Polarization Signals of Several Common Spacecraft Materials

June 1st, 1995

**Space Debris Research Group
Department of Aerospace
Engineering Science**

University of Colorado



**Colorado Center for Astrodynamics
Research (CCAR)**

Boulder, Colorado 80309-0431

(303) 492-6677

FAX (303) 492-2825



Polarization Signals of Several Common Spacecraft Materials

Culp, Robert D.¹ Gravseth, Ian²
King, Nicole³

Colorado Center for Astrodynamics Research
Department of Aerospace Engineering Sciences
University of Colorado
Boulder, CO 80309-0431

LOCKHEED ENGINEERING & SCIENCES CO.

Contracts NAG 9-768 and NAG 9-407

June 1st, 1995

¹Professor and Chairman

²NASA Graduate Student Research Fellow

³Undergraduate Research Assistant

List of Figures

2.1	Basic experiment setup	3
2.2	Direct light signal versus wavelength	4
B.1	Main Light Source Configuration	13
B.2	Basic Equipment Setup - Side View	14
B.3	Test Object Mount	14
D.1	Signal drop off versus off-axis viewing angle	17
D.2	Schematic of Double Glan Taylor Prism Polarizer	18
E.1	Light calibration results	20
H.1	Titanium Dioxide Sample	25
H.2	Steel Sample	25
H.3	Composite Sample	26
H.4	Kapton Sample; Aluminum Side	26
H.5	Kapton Sample; Copper Side	27
H.6	Insulating Foam Sample	27
H.7	Mylar Sample, smooth	28
H.8	Mylar Sample, wrinkled	28
H.9	Aluminum Sample	29
I.1	Mounting Schematic for Tether	31
I.2	Unblemished Tether Sample	32
I.3	Cut Tether Sample	32
I.4	Broken Tether Sample	33
I.5	Frayed Tether Sample	33
J.1	Albedo, Beta and Gamma Coefficients - Insulating Foam Sample	36
J.2	Raw Signal and Fit - Insulating Foam Sample	36
J.3	Albedo - MLI Sample	37
J.4	Raw Signal - MLI Sample	37
J.5	Albedo - TiO_2 Sample	38
J.6	Raw Signal - TiO_2 Sample	38
J.7	Albedo, Beta and Gamma Coefficients - Composite Sample	39
J.8	Raw Signal and Fit - Composite Sample	39
J.9	Albedo - Steel Sample	40
J.10	Raw Signal - Steel Sample	40

List of Tables

3.1	Polarization amplitudes, frequencies and phase shifts for materials tested .	7
J.1	Albedos, Gammas and Betas for materials tested	35

1	Introduction	1
2	Methodology	2
2.1	Procedure	2
2.2	Light Source	3
2.3	Spectrometer	3
2.4	Polarizer	5
2.5	Data Processing	5
3	Results and Discussion	6
4	Conclusions	8
4.1	Acknowledgements	8
4.2	References	8
A	Test Materials and Tasking	10
A.1	Materials Tested	10
B	Experimental Setup	12
B.1	Experimental Setup	12
C	Procedure	15
D	Equipment (Spectrometer and Polarizer)	16
E	Light Source	19
F	Object Handling	21
G	Data Processing	22
G.1	Measurements	22
G.2	Test Objects	22
G.2.1	Drift removal	23
G.2.2	Analysis of the Polarization data	23
H	Results	24
I	Tether Results	30
J	Albedo-Scattering Results	34

Abstract

This is the final report documenting the results of the polarization testing of near-planar objects with various reflectance properties. The purpose of this investigation was to determine the portion of the reflected signal which is polarized for materials commonly used in space applications. Tests were conducted on several samples, with surface characteristics ranging from highly reflective to relatively dark.

The measurements were obtained by suspending the test object in a beam of collimated light. The amount of light falling on the sample was controlled by a circular aperture placed in the light field. The polarized reflectance at various phase angles was then measured.

A nonlinear least squares fitting program was used for analysis. For the specular test objects, the reflected signals were measured in one degree increments near the specular point. Otherwise, measurements were taken every five degrees in phase angle.

Generally, the more diffuse surfaces had lower polarized reflectances than their more specular counterparts. The reflected signals for the more diffuse surfaces were spread over a larger phase angle range, while the signals from the more specular samples were reflected almost entirely within five degrees of angular deviation from the specular point.

The method used to test all the surfaces is presented. The results of this study will be used to support the NASA Orbital Debris Optical Signature Tests. These tests are intended to help better understand the reflectance properties of materials often used in space applications. This data will then be used to improve the capabilities for identification and tracking of space debris.

Chapter 1

Introduction

This is the final report documenting the polarization testing of near planar objects commonly used in spacecraft construction. This report is organized such that the main body contains only the most essential information; a more detailed description of each topic is then presented in an appendix. The testing methodology, laboratory setup, data reduction methods and results are briefly presented in the body of this report. The appendices contain more detailed descriptions of each of these sections. In addition, the appendices also contain information on the optical testing of a piece of tether material, and albedo-scattering information for the materials examined via the polarization experimentation.

Chapter 2

Methodology

The setup and procedure for the polarization of spacecraft materials testing was driven by the need to obtain accurate polarization measurements for a variety of phase angles. Measurements were taken over all possible phase angles where the reflected polarized signal was strong enough to detect. The spectrometer recorded data over the wavelengths from 347.7 nm to 1056.6 nm, although only a subset of this data was used in the final analysis.

With several objects to test, a spectrometer capable of efficiently collecting large numbers of measurements was required. The spectrometer used a 2 meter fiberoptic cable to transmit the recorded signals to the processing box. This cable allowed for enough mobility to take measurements at numerous phase angles. Appendix D contains additional information about the spectrometer.

In order to measure the polarized signal reflected off the samples an adjustable polarizer was interposed between the sensor and the test object. Only the reflected light with the correct polarization was allowed to pass through the polarizer to the sensor. The relative angle of the polarizer was adjustable down to tenths of a degree. More detailed information on the polarizer can be found in Appendix D.

Figure 2.1 shows the basic setup utilized in the testing. Appendix B contains more sketches and a discussion of the apparatus and setup.

figure 2.1

2.1 Procedure

Before the materials were tested, the experimental setup was aligned and tested. Several test runs through the experimental process were conducted. Materials that had been evaluated during previous tests were used as references. These tests of the set-up were conducted to ensure that the procedure was well rehearsed, and to flush out possible sources of error. Appendix F contains more information on the handling precautions implemented for the experiments.

After insuring that the set-up was working properly, the objects were placed in position and measurements were taken over all required angles in a timely manner. Dark measurements were taken approximately every five measurements in order to remove the drift present in the spectrometer's signal. This process was repeated for each test object until a sufficient amount of data was collected.

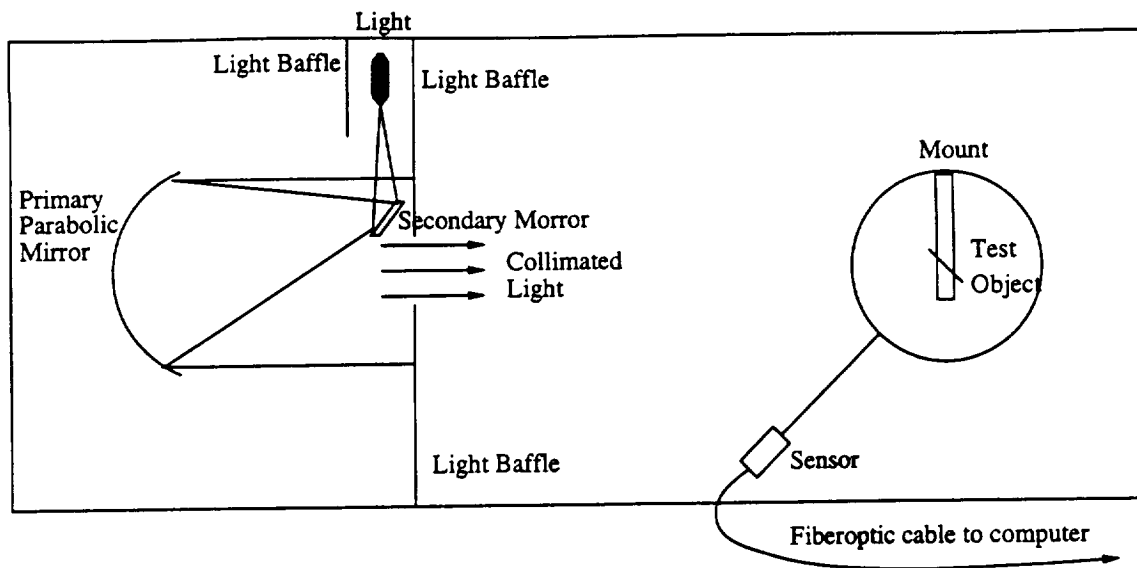


Figure 2.1: Basic experiment setup

2.2 Light Source

The test objects were illuminated by a 1000 Watt Quartz-Halogen source. The light produced was reflected onto a secondary mirror and from there onto the test object by a high precision parabolic mirror. The parabolic mirror had a 90 inch focal length, was 16 inches in diameter and had an angular deviation of about one half of a degree. This arrangement worked quite well, providing enough illumination for the spectrometer to work accurately within the range of wavelengths investigated. The direct light signal from the 1000W source is shown in figure 2.2.

2.3 Spectrometer

The spectrometer used during these investigations was supplied by Analytical Spectral Devices, Inc. (ASD) of Boulder Colorado. The LabSpec spectrometer was well suited to the conditions encountered during this study. This spectrometer was able to operate efficiently under the low light conditions encountered in the lab. The LabSpec was attached to a PC which drove the spectrometer and stored the data.

The LabSpec's greatest liability was the background noise present in its signal. The drift was measured during the testing and removed from the data afterwards. More detailed information on the spectrometer can be found in Appendix D. Information on how the drift was removed from the data can be found in Appendix G.

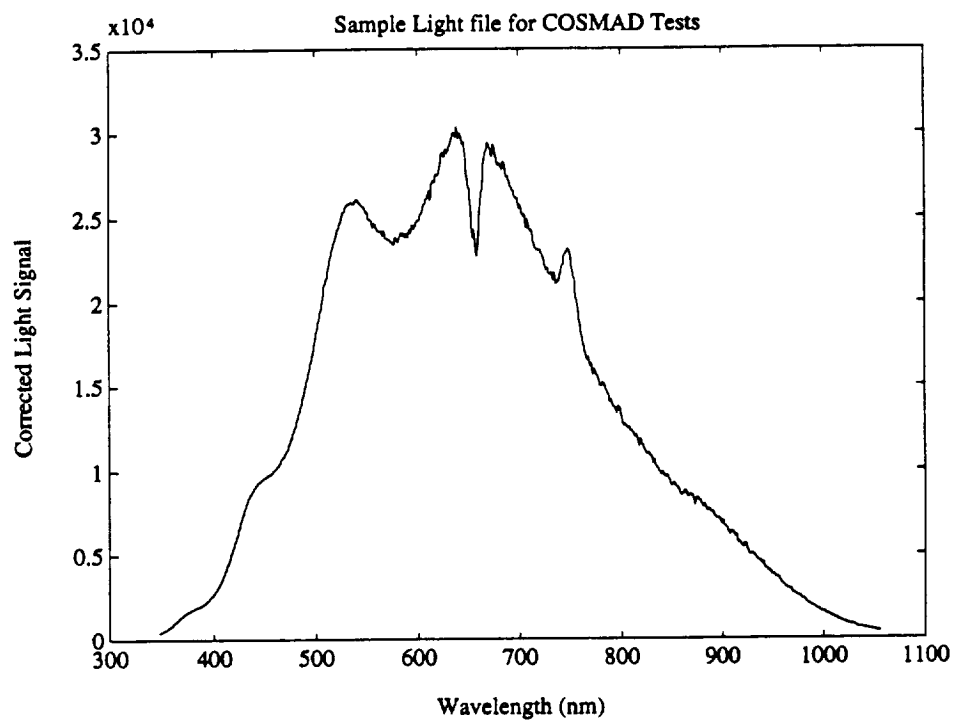


Figure 2.2: Direct light signal versus wavelength

2.4 Polarizer

The polarizer used in this experiment was manufactured by the Karl Lambrecht Corporation. Its orientation angle was controllable down to tenths of a degree.

2.5 Data Processing

Due to the large number of measurements necessary for each of the objects tested, the data were processed in two steps. Initially, programs were written to perform a preliminary analysis of the data from the objects at the laboratory site. If the results were reasonable, the data was transferred onto a UNIX system in the data processing center. At this location, the data were analyzed, plotted and tabulated. A detailed discussion on the data processing can be found in appendix G.

Chapter 3

Results and Discussion

This section contains the basic results of the study and a discussion of those results. The polarization versus phase angle plots along with the best fit plots for the materials tested are located in Appendix H.

The amount of polarization was found by taking the ratio of the difference and the sum of the perpendicular and horizontal polarizations. The equation used was

$$P = \frac{P_{\text{perp}} - P_{\text{horis}}}{P_{\text{perp}} + P_{\text{horis}}} \quad (3.1)$$

The polarization was found to vary sinusoidally with phase angle. The equation used to find the best non-linear fit for the data was:

$$y = A \cdot \sin(\omega \cdot \theta + \phi) \quad (3.2)$$

where

$$\begin{aligned} A &\equiv \text{amplitude} \\ \omega &\equiv \text{frequency} \\ \phi &\equiv \text{phase shift} \\ \theta &\equiv \text{phase angle} \end{aligned}$$

The values found for the amplitude, frequency and phase shift of this polarization data from this experiment, along with their deviations, are presented in Table 3.1. The amplitude of the corresponding sine wave gives an indication of the maximum amount of polarization possible for the material samples. The frequency shows how quickly the polarization changes with changing phase angle. The deviation values show how good the fit is for each specific variable.

The main errors in reducing the data seemed to be the drift of the spectrometer. The drift rate problem is discussed in detail in Appendixes D and G, but is outlined here. The spectrometer has a certain background noise which changes with temperature. As the temperature of the room fluctuates the background noise drifts. This was a problem because the drift rate over the cycle of measurements could be of the same magnitude as the actual measurements. In addition to the drift, there was also some random noise in the signal.

Material	Amplitude	σ	ω	σ	ϕ	σ
Titanium Dioxide	0.2400	0.1333	0.5401	0.4256	0.8232	0.2601
Steel	0.2275	0.0871	0.5263	0.1007	0.7790	0.1809
Composite	0.1825	0.0931	0.2685	0.1826	2.403	2.365
Kapton/Al side	0.4220	0.2146	0.5723	0.0697	5.347	0.5926
Kapton/Cu side	0.2681	0.1723	0.4780	0.1669	1.893	0.5926
Insulating Foam	0.0327	0.0271	0.0730	0.0437	3.156	1.619
Mylar, smooth	0.2590	0.0721	0.1155	0.0049	3.025	1.266
Mylar, wrinkled	0.0360	0.0172	0.2833	0.2174	1.402	0.920
Aluminum	0.4227	0.0918	0.6393	0.1292	2.933	1.214

Table 3.1: Polarization amplitudes, frequencies and phase shifts for materials tested

Many measurements were made of the drift rate for the spectrometer. This drift rate could be effectively removed for the wavelengths with the stronger signals. Due to the much smaller light strength at the extreme wavelengths, however, the errors at these wavelengths were expected to be higher and were, consequently, not used.

Chapter 4

Conclusions

The methodology and results for the polarization testing have been presented. The results obtained in this testing are contained in table 3.1. Generally, the surfaces with a highly specular nature had relatively large polarization signals, while the more diffuse surfaces had much lower polarization signals. Additionally, information on the albedo-scattering characteristics of the materials tested during the polarization testing are contained in Appendix J. Also, information on the albedo-scattering testing performed on a piece of tether material is contained in Appendix I.

4.1 Acknowledgements

The authors would like to acknowledge the contributions of Dr. William McClintock of the Laboratory for Atmospheric and Space Physics (LASP) for the use of his laboratory, equipment and time, and David Hatchell of Analytical Spectral Devices (ASD) for help with the spectrometer. The authors would also like to thank Erika Norman-Gravseth, of Ball Aerospace for her assistance in obtaining some of the materials which were tested in these experiments.

4.2 References

- Allen, C.W. Astrophysical Quantities. Third Ed., The Athlone Press, London, 1973, pg. 108.
- CRC Handbook of Chemistry and Physics, 62nd Ed, CRC press, Boca Raton, 1981, pg E-386.
- Egan, W.G. and T. Hilgeman. *Applied Optics*, Vol. 15, No. 7, July 1976, pp. 1845-1849.
- Egan, W.G. and T. Hilgeman. *Applied Optics*, Vol. 16, No. 11, November 1977, pp. 2861-2864.
- Hapke, B. and E. Wells, "Bidirectional Reflectance Spectroscopy I - Theory", *Journal of Geophysical Research*, Vol 86, No B4, April 10, 1981, pp 3039-3054.

- Hapke, B. and E. Wells, "Bidirectional Reflectance Spectroscopy II - Experiments and Observations", *Journal of Geophysical Research*, Vol 86, No B4, April 10, 1981, pp 3055-3060.
- Lompado, A., B.W. Murray, J.S. Wollam, and J.F. Meroth, "Characterization of optical baffle materials." *SPIE Proceedings Series: Scatter from Optical Components*, Vol. 1165, 1989, pp. 212-226. Proceedings of a conference, 8-10 August, 1989, San Diego, CA.
- Madler, R.A., R.D. Culp, and T.D. Maclay. "ODERACS II pre-flight optical calibration." To be presented as the 1993 SPIE Aerospace and Remote Sensing Conference, Orlando, Florida, 12-16 April, 1993, Paper 1951-06.
- Marx, E. and T.V. Vorburger. "Light scattered by random surfaces and roughness determination." *SPIE Proceedings Series: Scatter from Optical Components*, Vol. 1165, 1989, pp.72-86. Proceedings of a conference, 8-10 August, 1989, San Diego, CA.
- Press, W.H., B.P. Flannery, S.A. Teukolsky, and W.T. Vetterling. Numerical Recipes: The Art of Scientific Computing. Cambridge University Press, Cambridge, 1986.
- Ramhauske, W.R. and R.R. Gruenzel. *J. Am. Opt. Soc.*, Vol. 55, No. 3, March 1965, pp. 315-318.
- Stover, J.C. Optical Scattering: Measurements and Analysis. McGraw-Hill, N.Y., 1990.
- Veverka, J. "Photometry of Satellite Surfaces," in Planetary Satellites, ed. Joseph Burns, University of Arizona Press, Tucson, 1977.
- Henninger, J. H. "Solar Absorptance and Thermal Emittance of Some Common Spacecraft Coatings," *NASA Reference Publication 1121*, April 1984.

Appendix A

Test Materials and Tasking

A.1 Materials Tested

This section contains a description of the materials that were tested during this investigation. Included are a description of the material, visual observation about the surface, and any other unique information about a given sample.

- Titanium Dioxide

The Titanium Dioxide sample tested was approximately 12 cm X 4 cm. It was painted upon one side of a metallic plate. Visual inspection indicated that the sample had a large specular and a large diffuse component.

- Steel

The steel sample tested was 302 stainless steel and was approximately 12 cm X 4 cm in cross sectional area. Visual inspection indicated that the majority of its signal was specular.

- Composite

The composite sample tested was approximately 6 cm X 4 cm. Qualitatively its coloring was nearly black, but a large portion of its reflected signal appeared to be specular. Visual inspection indicated that its albedo was lower than many of the other samples tested.

- Kapton

The Kapton sample was silver on one side and copper on the other. Visual inspection indicated that most of its reflected signal for both sides was specular.

- Insulating Foam

The insulating foam tested was similar to styrofoam in appearance. The sample tested was designed for insulating antennae from noise. Visual inspection indicated that the majority of its reflected signal was diffuse.

- Mylar with polyester net

The Mylar with polyester net sample consisted of a sheet of mylar covered by a loose polyester net. The sample was highly reflective, and most of the reflected signal was specular in nature.

- Aluminum

The aluminum sample has a dull mirrorlike appearance. The surface is shiny and reflects light well, but it is not polished enough to see clear images reflected on the surface.

Appendix B

Experimental Setup

B.1 Experimental Setup

The purpose of this experimental setup was to simulate as closely as possible the solar radiation incident upon an object in orbit about the Earth in order to estimate the reflectance characteristics for several objects. The light used was collimated (parallel light rays) and controlled to fall only on the object that the spectrometer was measuring. All other light was blocked out by means of baffles, see sketches. The light source used was a 1000-watt bulb with a constant power supply, see Appendix E. It was collimated using a parabolic mirror placed at one end of the experimental table. The light source was placed at a distance equal to the parabolic mirror's focal length, 90 inches. Due to space constraints, it was necessary to place the light source to the side of the table. The beam was aimed at a 4 inch flat mirror that was used to reflect the beam into the mirror. The distance from the bulb to the flat mirror and the flat mirror to the parabolic mirror was 13 and 77 inches respectively.

Extraneous light was the greatest concern while running this experiment. Many measures were taken to absorb and block all light except that which fell on the test object. The experiment was conducted in a black-painted room with all outside light sealed out. The baffles used were carefully fit together and covered with black felt, forming a large black box in which the light source was placed. This allowed only a simple beam of light to emerge past the baffles. However, the parabolic mirror was not enclosed due to its distance from the source. This was the main source of extraneous light.

The mount itself had a built in angular protractor, making angle measurements quick and accurate. The mount stood 11 inches high and was covered with black felt. Attached to the mount was a bracket measuring 16 inches in height from which suspended the test objects. Attached to the side of the mount was an extended arm used to hold the spectrometer sensor.

The test objects were held by four clamps that were suspended from the bracket frame. These clamps were attached to the four corners of the piece, which were typically rectangular in shape, and held the piece suspended vertically in the light beam. This frame also allowed for the pieces to be placed at various angles with respect to the light field. The measurements for this experiment were taken with the test object located at 20 and 30 degrees with respect to the normal of the incident light.

A polarizer was placed between the sensor and the test sample. It was affixed to the

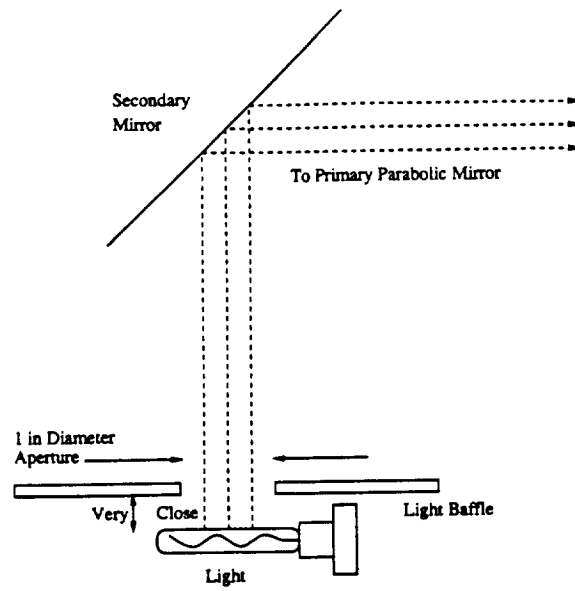


Figure B.1: Main Light Source Configuration

same arm as the sensor. During the testing, it was placed at orientations of zero and ninety degrees. Additional information is included about the polarizer in Appendix E.

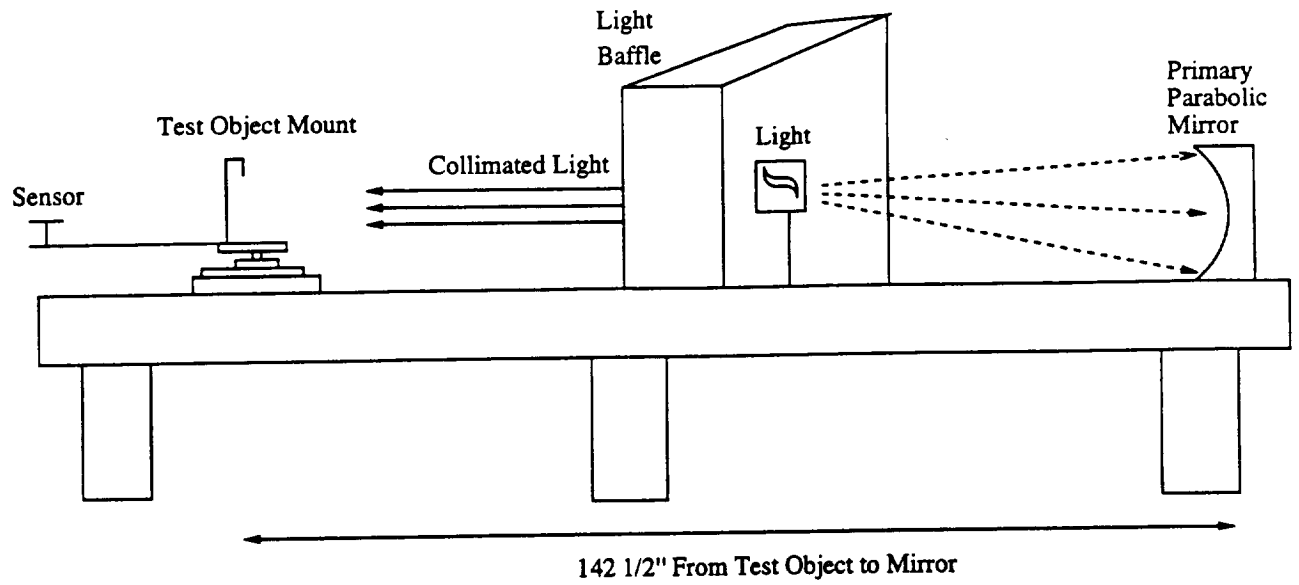


Figure B.2: Basic Equipment Setup - Side View

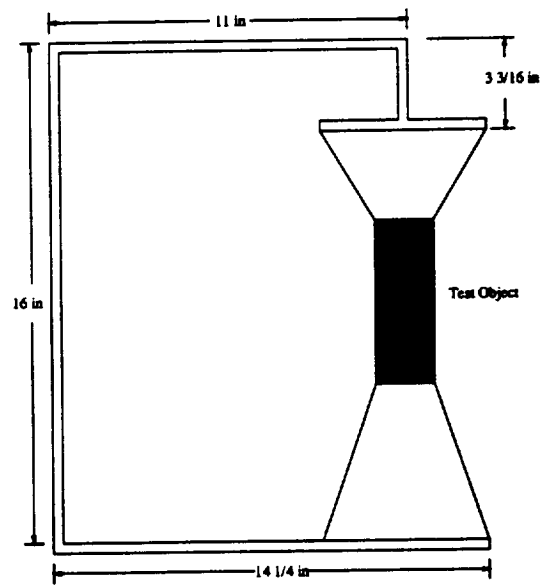


Figure B.3: Test Object Mount

Appendix C

Procedure

Each day before testing, the laboratory equipment used in this experiment was set up and aligned. The power supply and the light source were turned on immediately so they could warm up, which helped to minimize variations in the light beam. After the lab was set up and properly aligned, the test object was mounted on the frame. Clamps held the piece at four corners to suspend it vertically in the light beam. The material was viewed from the side and visually adjusted to assure it was centered on the angular protractor and its normal lay the same plane as the incident light and the sensor. The sensor was then mounted and aligned to point at the specular point of the test article. The polarizer's alignment was also checked.

After rechecking the mount and experimental set-up, all lights were extinguished and an appropriate integration time was chosen for the set of measurements. For the more diffuse surfaces these measurements were usually taken in 5 degree increments, starting at -35 degrees and going to 110 degrees with respect to the incident light. For each phase angle one measurement was taken for the vertical and horizontal polarization. For the more specular objects were analyzed more closely with finer increments of measurements taken near their specular point. Generally the observations were taken in one degree increments when within twenty degrees of the specular point. Again, for each phase angle measurements at two perpendicular polarizations were recorded. The angular protractor allowed accurate measurements of the sensor angle down to fractions of a degree. Before or after a set of measurements was taken on a test object, the direct light signal was measured.

The polarizer also allowed the polarizer's angle to be recorded down to tenths of a degree. When the measurements were completed, the sample was taken down and put back in its Ziploc bag. The data from the spectrometer was graphically analyzed and transferred to floppy disk for future analysis.

Appendix D

Equipment (Spectrometer and Polarizer)

Spectrometer

The spectrometer used for this laboratory experiment was a LabSpec, designed and built by Analytical Spectral Devices, Inc. (ASD) of Boulder. It has 512 channels for data sampling, utilizing a plasma coupled photodiode array, with spectral range of 347.7 to 1056.6 nm. It has integration times ranging from 17 milliseconds to nine minutes. The spectrometer's noise can be removed either manually or automatically. The sensor utilizes fiber optics, and it has a two meter cable so that the sensor can be easily moved. The sensor itself consists of a fiber optics bundle that is roughly 0.6 mm in diameter at its terminus.

Although on the whole the spectrometer was well suited for this experiment, its recorded signal had a significant amount of drift in its dark signal over time, partially due to temperature fluctuations within the room. While this drift would be relatively insignificant for measurements being taken under sunlight, with this laboratory experiment the amount of noise in the signal was significant, especially when viewing the test article with long integration times and small reflected signals.

Since the signal had a significant drift in it, the drift was subtracted from the signal by assuming that the drift between two successive dark measurements was linear. This provides an acceptable estimation of the signal for the wavelengths with a strong signal, but causes the extreme wavelength calculations to be unreliable. For this reason the extreme wavelengths have not been used in the calculations.

Procedures to allow for the careful aiming of the sensor were developed. This was necessary due to the signal falloff at angles offset from the bore sight. This signal falloff as a function of off-axis angle is shown in Figure D.1. However, for the diffuse objects a significant signal comes from the off-bore sight directions. For this reason, these objects were viewed from as great a range as possible to reduce the maximum off-axis angle.

Polarizer

The polarizer utilized in this set of experiments was provided by the Laboratory of Atmospheric and Space Physics. The polarizer was the Double Glan Taylor Prism Polarizer, and it was manufactured by the Karl Lambrecht Corporation. The angle of the polarizer was

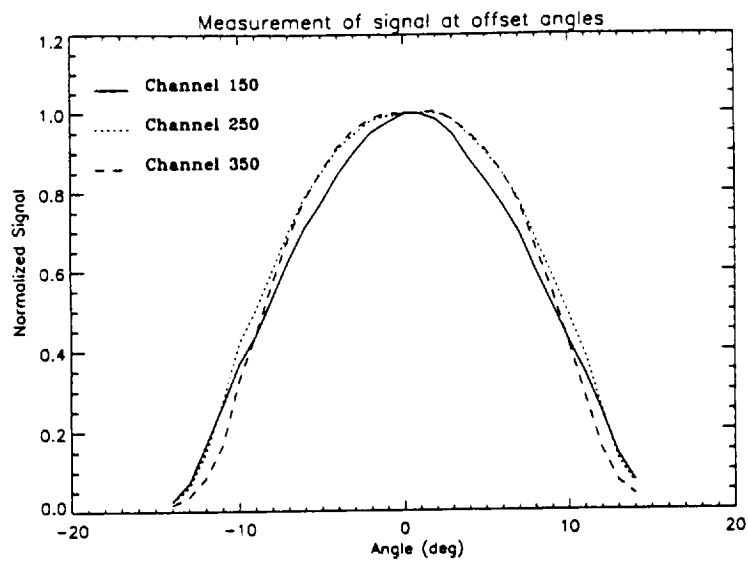


Figure D.1: Signal drop off versus off-axis viewing angle

adjustable by rotating a dial in which the polarizer was set. The angle of the polarizer could be adjusted down to tenths of degrees. A diagram of the polarizer is shown in figure 2.

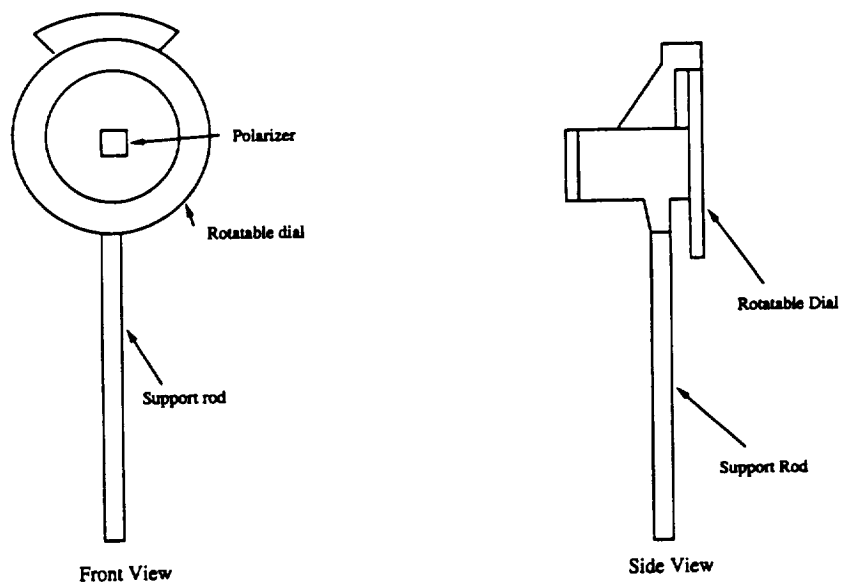


Figure D.2: Schematic of Double Glan Taylor Prism Polarizer

Appendix E

Light Source

All the objects were illuminated with a 1000 Watt Quartz-Halogen light source reflected through a high precision parabolic mirror to form a highly collimated light beam which closely resembles actual solar conditions. The lamp was a commercial GE type FEL 1000-watt lamp having a tungsten coiled-coil filament enclosed in a small quartz envelope. The focal length of the Parabolic mirror was 90 inches. The resulting beam has divergences ranging between 0.5 and 0.7 degrees, based on and limited to the accuracy of the actual beam projection dimension measurements. This compares well with the actual sun conditions of 0.53 degrees. See Appendix B where Figures B.1 and B.2 show the setup of the light source.

This lamp was powered by a constant power supply source which provides a constant 8 amperes of current to the light. Figure 2.2 shows the raw data from a direct measurement of the light. This signal shows the spectrum of the light source as sensed by the spectrometer. This can be compared with the calibration of another light bulb of the same model performed by Optronics Laboratories, Inc. The spectral irradiance is given in $\frac{\text{microwatts}}{\text{cm}^2 \text{nm}}$ at a distance of 50 cm when the light is operated at 8.0 amperes. ¹ The differences between Figs. 2.2 and E.1 are most likely due to spectrometer characteristics and some variance in the signal produced by each bulb.

¹Letter from Optronics Lab dated 19 March, 1986

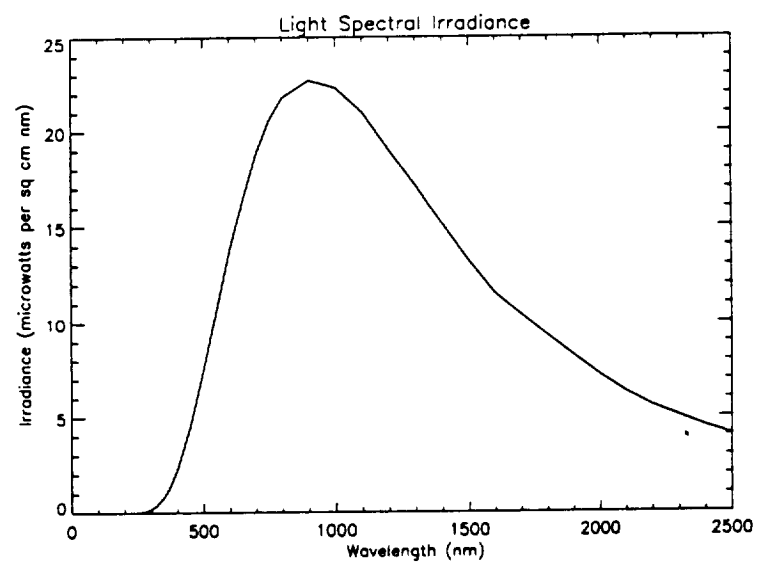


Figure E.1: Light calibration results

Appendix F

Object Handling

The objects used in this investigation were all handled with care. The intent of this study was to investigate the test objects' reflectance characteristics, so all reasonable steps were taken to assure that the test objects' surfaces were not altered. All handling procedures were rehearsed before the test articles were removed from their cases. As a result of the rehearsal, the experiments proceeded smoothly without incident.

Appendix G

Data Processing

This section describes the methodology used in the data processing. The following is a listing of the basic steps that were used in order to analyze the polarization data.

Data Processing Procedure

1. Take polarization measurements
2. Quick analysis of results on a PC
3. Transfer data to a UNIX system for in-depth analysis
4. Tabulate and plot results

G.1 Measurements

As mentioned before, the spectrometer stores information for each of its 512 channels at each phase angle. Measurements were taken from one to five degree intervals for all possible angles. The variation in the angle increment size was determined in order to accurately model the reflectance of the test objects and determine the polarization estimates. The reflectance data was saved and quickly analyzed on the PC. A backup copy of the data was saved on floppy disks for storage. Finally, the data files were transferred to a UNIX system for complete analysis, tabulation and plotting.

G.2 Test Objects

This section discusses the data analysis for the test objects. The analysis consisted of 7 test objects as described in detail in appendix A. The polarization for the test objects was calculated using the equation:

$$P = \frac{P_{\text{perp}} - P_{\text{horiz}}}{P_{\text{perp}} + P_{\text{horiz}}} \quad (\text{G.1})$$

After plotting the polarization results versus phase angle, a sinusoidal relationship was discovered. Values for the sinusoidal variables were obtained by first estimating the values of its amplitude, frequency and phase shift from the test data. Using a FORTRAN based computer program, the estimation of the three values were calculated fairly rapidly using

a limited set of data. Numerical nonlinear fitting techniques were used to find the best fit values for the amplitude, frequency and phase shift for the polarization with respect to phase angle.¹

G.2.1 Drift removal

A characteristic of the spectrometer that had to be considered when analyzing the data was the drift or internal noise in the spectrometer signal. The drift produced by the spectrometer was influenced by the room's temperature and the spectrometer's circuitry. Other unidentifiable factors may have also contributed to the spectrometer's drift. After every five data readings, a "dark" signal reading was taken. This dark signal represented the ambient or internal noise of the spectrometer at the time the data was taken. By constructing a linear fit between each dark signal, it was possible to remove the noise from each data point. This noise removal improved the quality of the measured reflected signal significantly. The linear fit between dark points as well as the noise removal from the data points was carried out by a computer program. The drift was assumed to vary linearly between dark signals with the following equation:

$$D = D_0 + \partial D \cdot t \quad (\text{G.2})$$

$$\partial D = \frac{D_0 - D_1}{t_0 - t_1} \quad (\text{G.3})$$

G.2.2 Analysis of the Polarization data

A FORTRAN program was written to analyze the data after the measurements were taken to find the percent of polarization. This program follows the outline seen below.

polarization analysis

1. Read in the light signal.
2. Read in the measurements at different phase angles.
3. Correct for the spectrometer's drift.
4. Calculate the polarization at each angle using equation .
5. Plot results on the monitor and store the data for more plotting later.

¹Press, W., Teukolsky, S., Vetterling, W., Flannery, B. 1992, Numerical Recipes New York, NY: Cambridge University Press

Appendix H

Results

This section discusses the results of the polarization tests and shows the best fit versus real data curves for each sample. Plotting the percent of polarization versus phase angle, there appeared to be a sinusoidal relationship. A non-linear least squares fitting program was used to approximate this relationship. This is discussed further in appendix G.

The plots of the fitted data are attached. The dotted line represents the real data while the solid line is the best fit approximation. The amplitude of the fitted sine wave gives an indication of the maximum amount of polarization possible.

Two plots are shown for the mylar test sample. This is because of the large differences in the two examples. In the first graph, the mylar was stretch tightly in the mount to assure that there were no wrinkles. In the next one, the mylar was not as taut and consequently had some wrinkles in it. This greatly affected the results. In the first instance, the frequency of the corresponding sine wave was much smaller than in the other. This is believed to be caused by the wrinkles in the material causing the polarized light rays to hit each other at different angles. This could cancel or increase the polarization in the reflected light signal, causing the percent of polarization to change more rapidly with varying phase angle.

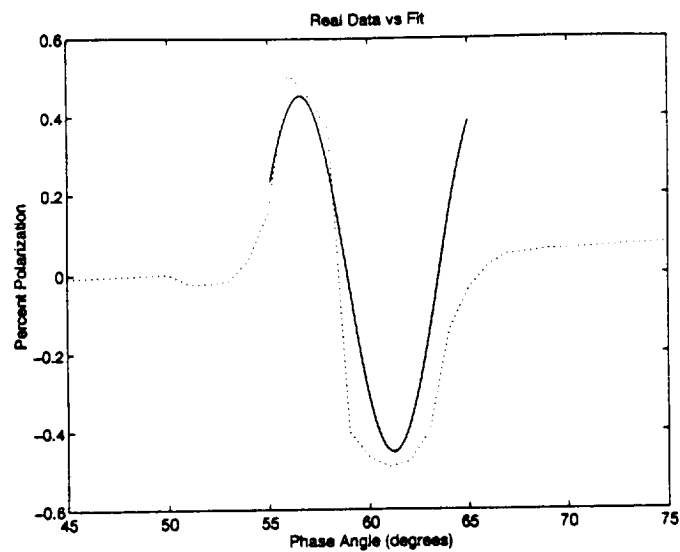


Figure H.1: Titanium Dioxide Sample

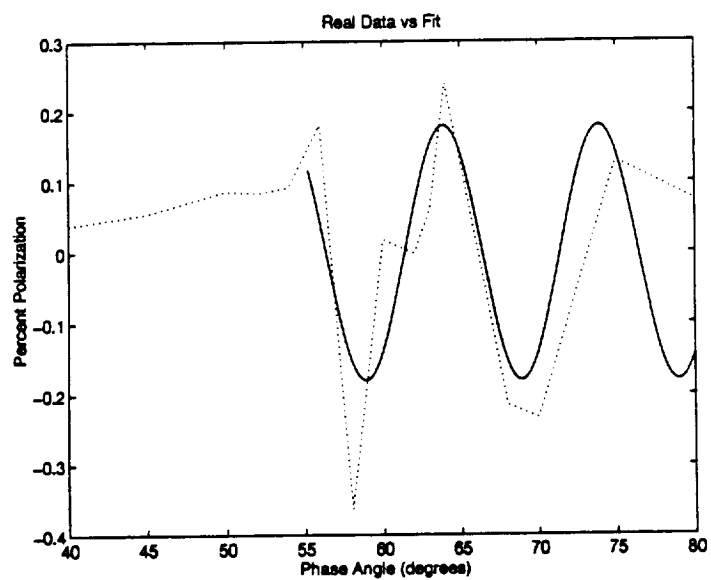


Figure H.2: Steel Sample

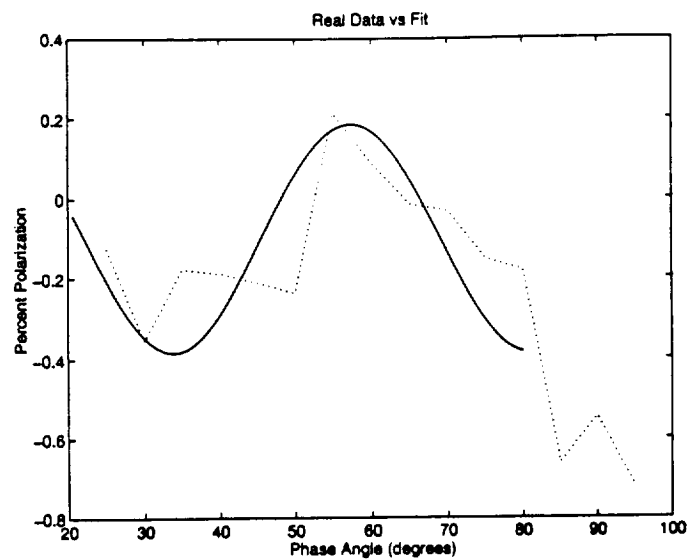


Figure H.3: Composite Sample

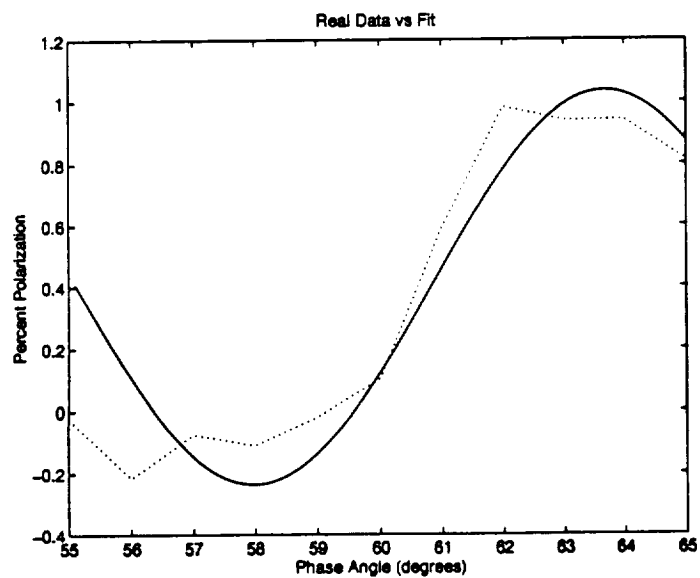


Figure H.4: Kapton Sample; Aluminum Side

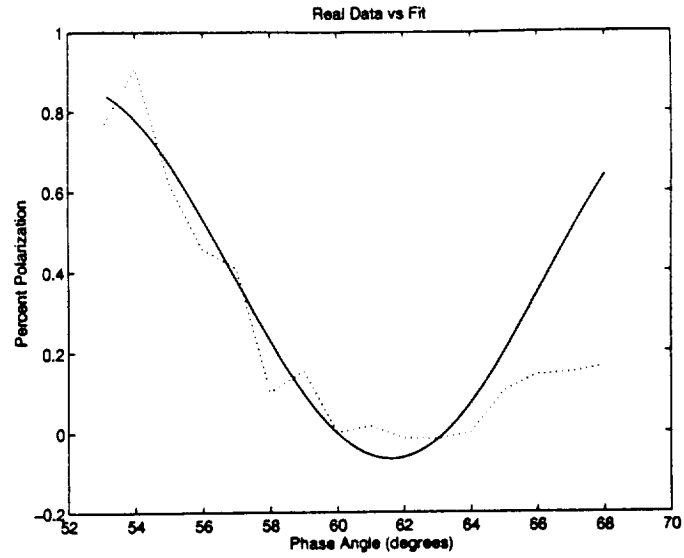


Figure H.5: Kapton Sample; Copper Side

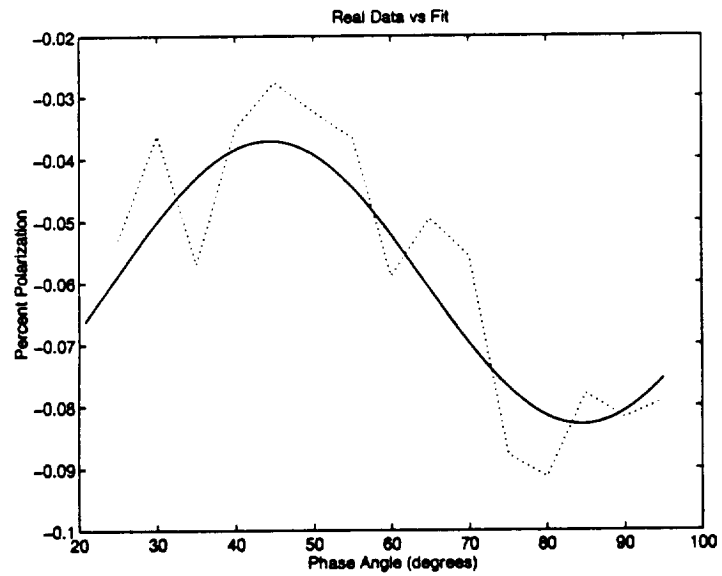


Figure H.6: Insulating Foam Sample

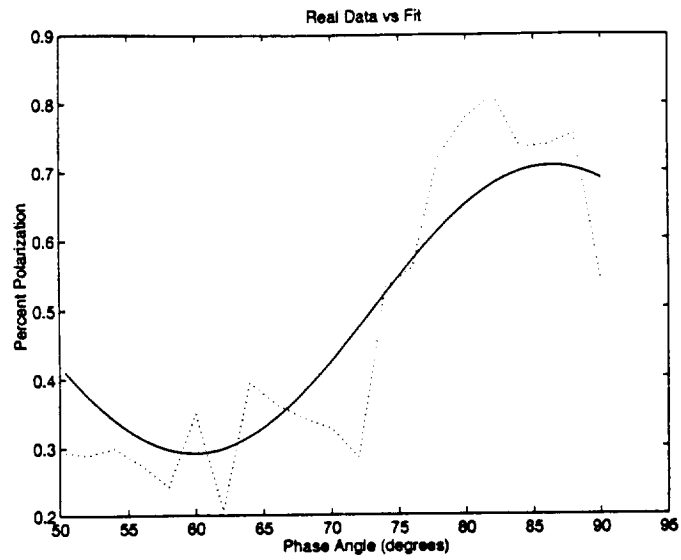


Figure H.7: Mylar Sample, smooth

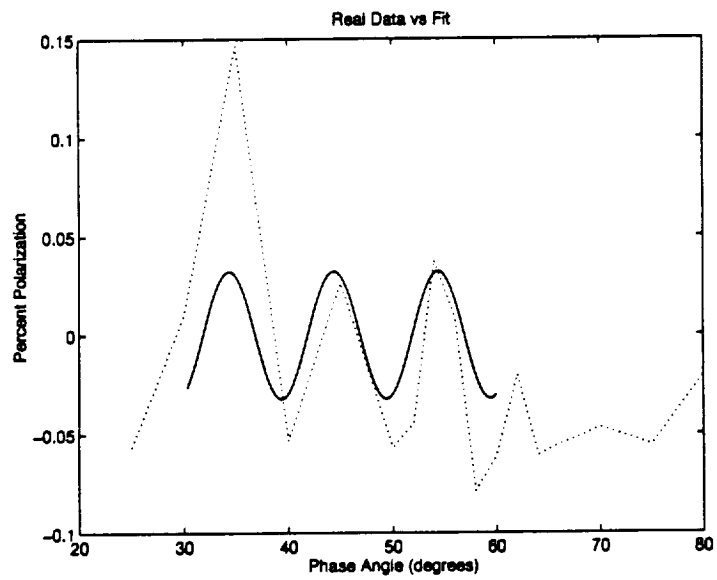


Figure H.8: Mylar Sample, wrinkled

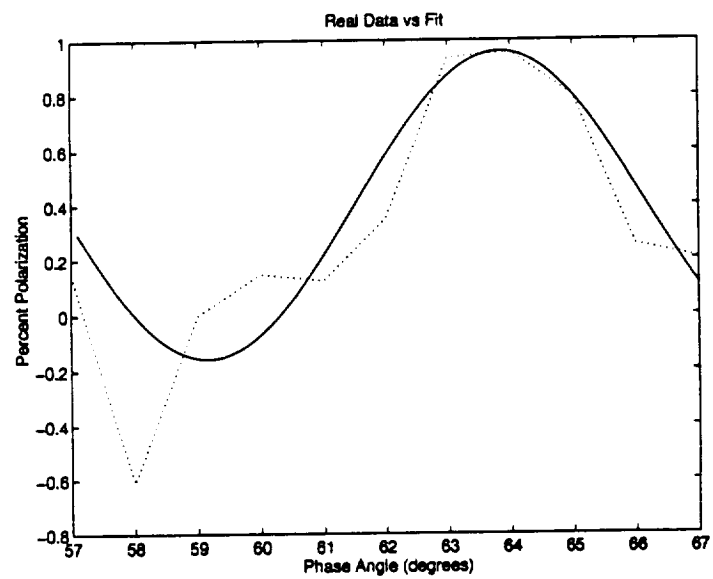


Figure H.9: Aluminum Sample

Appendix I

Tether Results

This section contains information on the optical testing of tether material. In a general sense, the testing conducted on the tether material was performed in a manner similar to that which was performed in the albedo-scattering testing of the common spacecraft materials. Other than the tether being mounted in a slightly different manner, the experimental setup was identical to the albedo-scattering testing. The tether mount is shown below.

The tether was suspended within the light field and clamped at each of its ends by a pair of alligator clamps.

Also, a slightly different range of phase angles was covered in this portion of the testing. Since the sample itself did not block the reflected signal at phase angles greater than 135 degrees, measurements could be taken past that point. Generally measurements were taken over phase angles ranging from as near zero degrees to as near 180 degrees as was possible.

subsection*Creation of tether pieces The original tether sample was broken and cut to simulate how it would look if it were broken or partially damaged by a piece of debris. The cut tether was created by partially severing the tether with a razor blade. A broken tether sample was created by shooting a portion of the tether with a .22 pistol. Although some of the initial shots simply bounced off the tether, one of the later ones succeeded in severing it. The broken pieces were then analyzed within the laboratory. subsection*Results

The tether data was collected on a PC and later transferred to a Unix system where it was analyzed in greater detail. After subtracting the dark signal from the recorded signals, the normalized reflected signal was then least squares fit to an equation of the form:

$$\frac{E_r}{E} = A((\gamma \frac{\tau h}{2} \pi R^2)(\sin(\theta) + (\pi - \theta)\cos(\theta)) + (1 - \gamma)\frac{r}{2R}\cos(\theta/2)) \quad (I.1)$$

E_r	\equiv	Reflected flux
E	\equiv	Incident flux
R	\equiv	Radius of Sensor
τ	\equiv	Radius of Cylinder
h	\equiv	Height of Cylinder
a	\equiv	Albedo
γ	\equiv	Percentage of Light Scattered Diffusely
θ	\equiv	Phase Angle (radians)

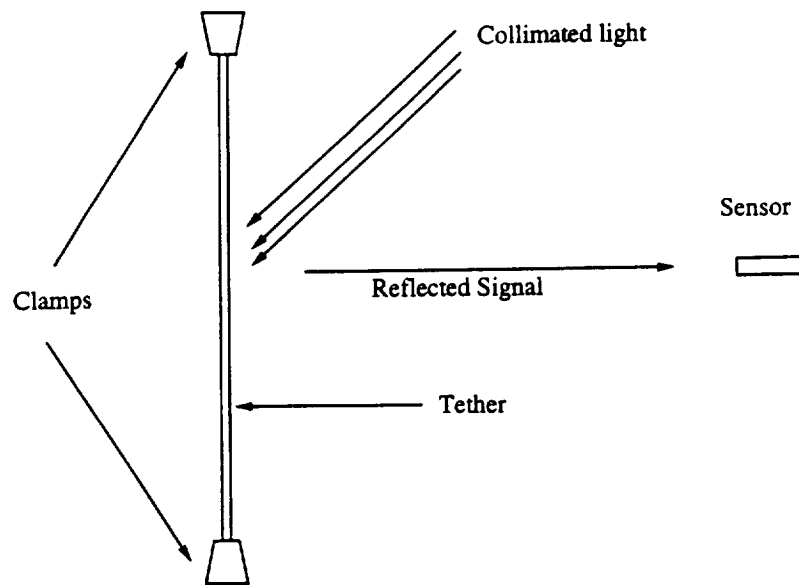


Figure I.1: Mounting Schematic for Tether

Four different tether types were conducted on four different tether types. An undamaged tether, a cut tether, and two cases of broken tether. The first broken tether sample was a clean break, and the second one analyzed was a rough break – the tether material was pulled apart in this case. Unfortunately, the specular-diffuse cylindrical model was a poor choice for the tether sample. In the cases which involved a broken or cut tether, a large signal was transmitted through the tether material. Below are shown the phase functions for the various samples which were tested.

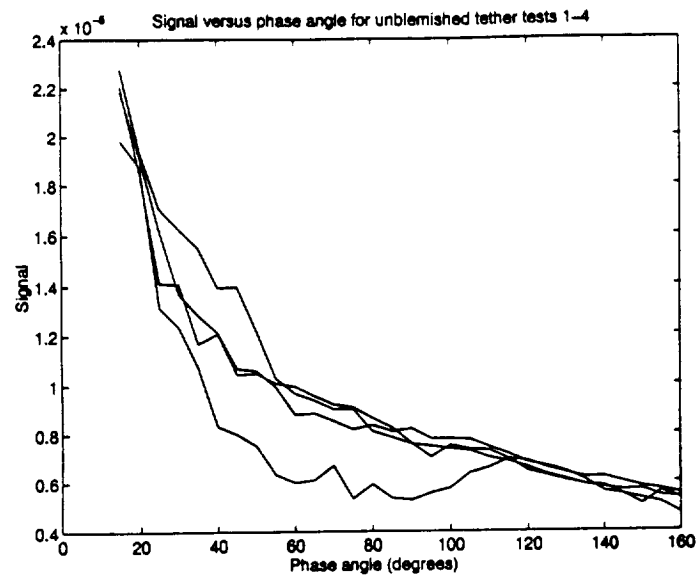


Figure I.2: Unblemished Tether Sample

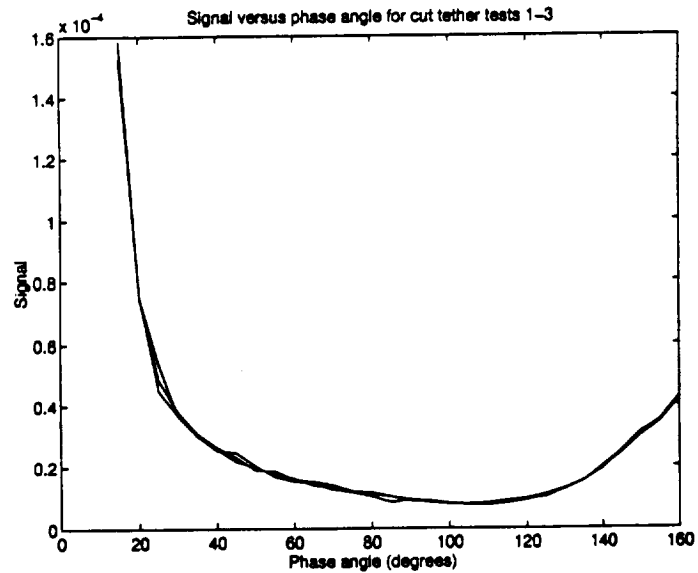


Figure I.3: Cut Tether Sample

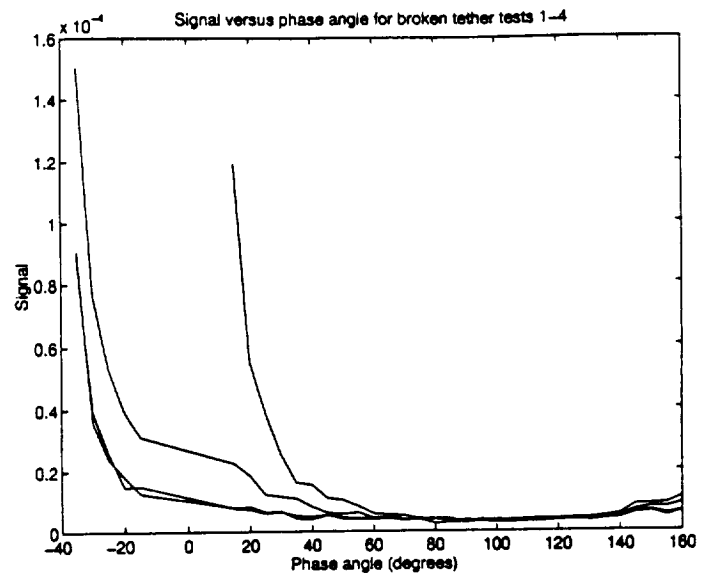


Figure I.4: Broken Tether Sample

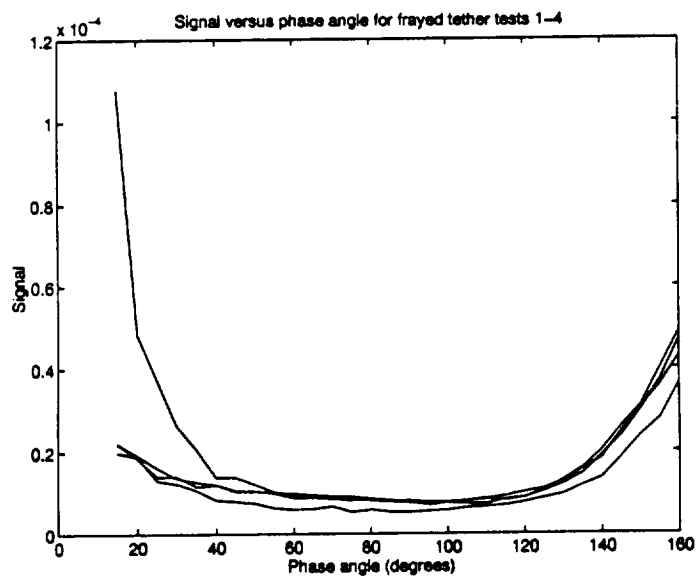


Figure I.5: Frayed Tether Sample

Appendix J

Albedo-Scattering Results

This appendix discusses the albedo-scattering results for the common spacecraft materials which were tested. A brief description of the experimental setup, the analysis and the results obtained are presented here. For a more complete description of this type of experiment please refer to "Common Spacecraft Material Debris - Final Report", Report to Lockheed.

Experimental Setup

The setup and procedure for this testing was driven by the need to obtain both scattering and specular measurements for a variety of surfaces at numerous phase angles. The setup was also designed with the intention of simulating as closely as possible the conditions which would be experienced by a piece of orbiting debris. The physical setup of the experimental setup for this test was identical to that of the polarization testing, except that the polarizer was not placed in front of the sensor – the sensor received the raw reflected light signal.

Procedure

After aligning the equipment and allowing the light source and spectrometer to warm up for a sufficient amount of time the actual testing of the samples began. Measurements on the more diffuse samples were generally taken over phase angles ranging from -35 degrees to 110 degrees in 5 degree increments. For the specular samples, when near the specular point measurements were taken in one or two degree increments. Also, as the testing progressed the dark current within the spectrometer was recorded approximately every five measurements. The direct light current was also recorded either at the beginning or the end of the test.

Generally, each sample was tested multiple times once it was aligned on the test stand.

Analysis of Data

Prior to fitting least squares fit curves through the data, the dark signal was subtracted from the recorded signals and each signal was normalized by the recorded light signal. The resulting data was least squares fit to an equation of the following form:

$$\frac{E_r}{E} \cdot \frac{R_s^2}{r_A^2} = a \cdot [\gamma \cdot \cos(\rho) + \beta \cdot b \cdot e^{-\eta} + (1 - \beta - \gamma) \cdot d \cdot (1 + \cos(f \cdot \eta))] \quad (J.1)$$

Material	Albedo	σ	β	σ	γ	σ	c	f
Aluminum	0.754	0.0970	1.0	-	0.	-	-	-
Insulating Foam	.509	.0055	.00023	.00032	.962	.0482	18.0	3.0
MLI	.984	-	1.	-	0.	-	12.0	-
TiO_2	0.818	0.0810	1.0	-	0.0	-	-	-
Composite	.250	.0117	.00956	.00088	.537	.0479	18.0	3.0
Steel	.6	-	1.	-	0.	-	12.0	-

Table J.1: Albedos, Gammas and Betas for materials tested

$$\rho = |\theta - i| \quad (J.2)$$

$$\eta = |2 \cdot i - \theta| \quad (J.3)$$

- $E_r \equiv$ Reflected flux
- $E \equiv$ Incident flux
- $r_A \equiv$ Radius of Illuminated Area
- $R_s \equiv$ Radius of Sensor
- $a \equiv$ Albedo
- $\gamma \equiv$ Percentage of Light Scattered Diffusely
- $\beta \equiv$ Percentage of Light Scattered Specularly
- $(1 - \beta - \gamma) \equiv$ Percentage of Directionally Scattered Light
- $\rho \equiv$ Angle Between Normal and Reflected Light
- $\eta \equiv$ Angle Between Specular Point and Reflected Light
- $b \equiv$ Specular Normalization Coefficient
- $d \equiv$ Directional Scatter Normalization Coefficient
- $c \equiv$ Exponential Estimate
- $f \equiv$ Directed Scatter Factor
- $\theta \equiv$ Phase Angle
- $i \equiv$ Test Object's Inclination

For some of the highly specular samples, a direct integration method was utilized to determine their albedos.

Experimental Results

Several tests were performed on each piece tested to insure that the results obtained were sufficiently accurate. The table shown below lists all of the results obtained.

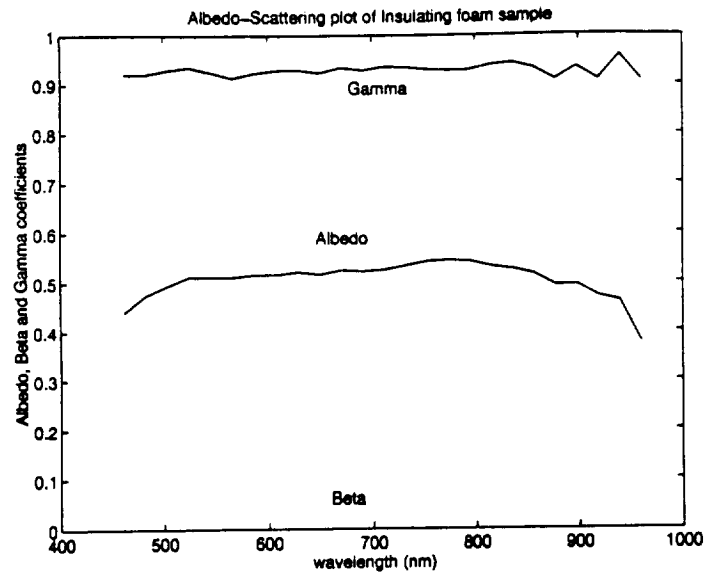


Figure J.1: Albedo, Beta and Gamma Coefficients - Insulating Foam Sample

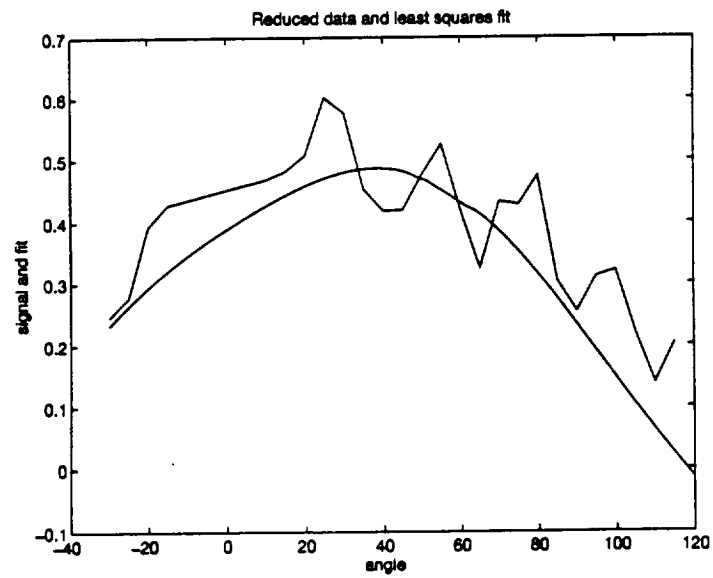


Figure J.2: Raw Signal and Fit - Insulating Foam Sample

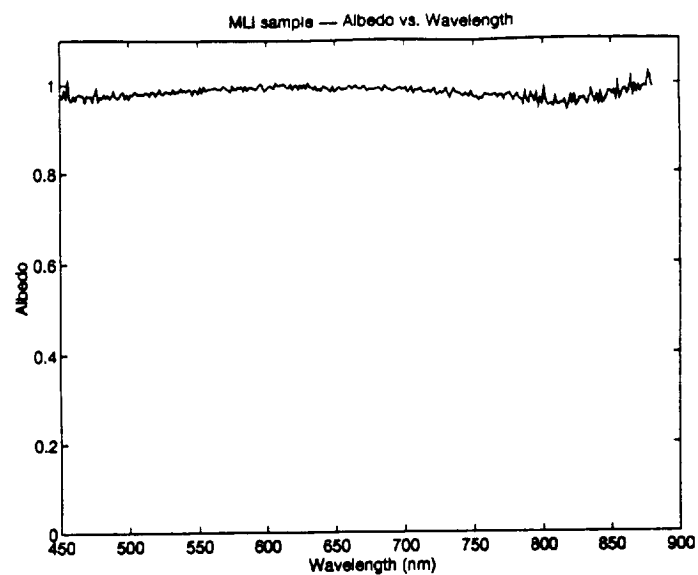


Figure J.3: Albedo - MLI Sample

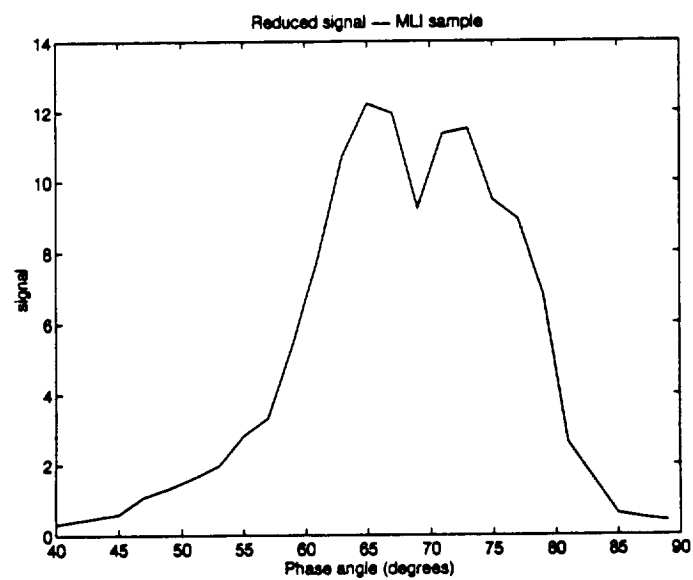


Figure J.4: Raw Signal - MLI Sample

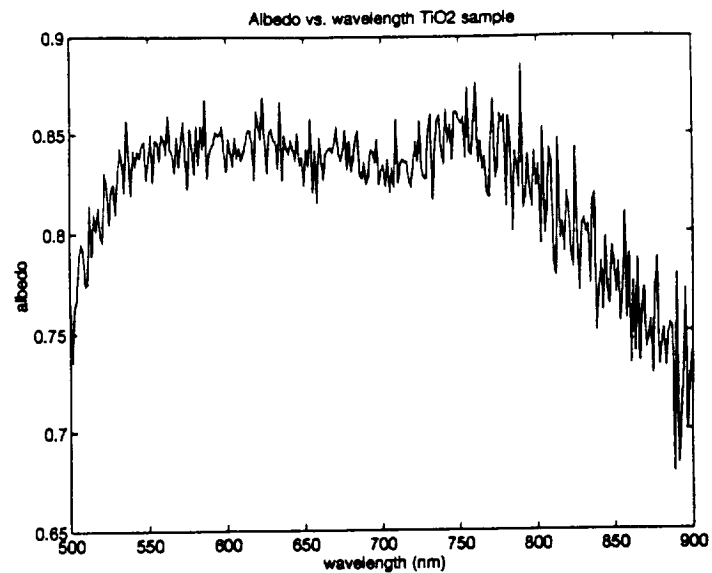


Figure J.5: Albedo - TiO_2 Sample

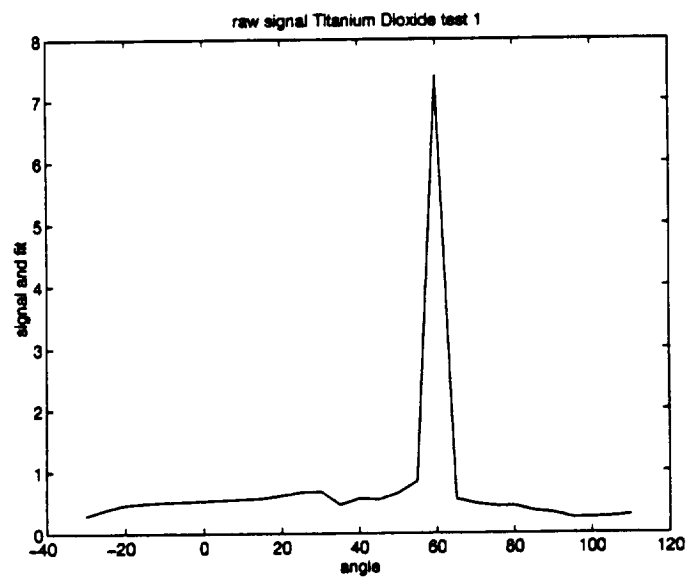


Figure J.6: Raw Signal - TiO_2 Sample

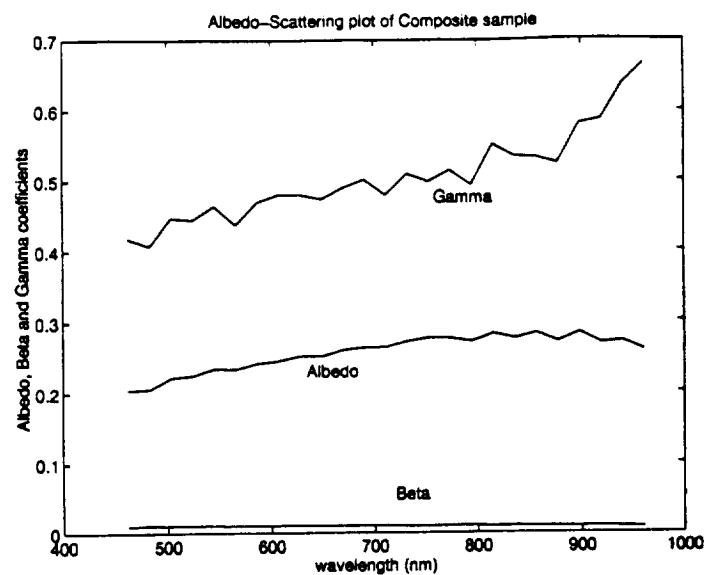


Figure J.7: Albedo, Beta and Gamma Coefficients - Composite Sample

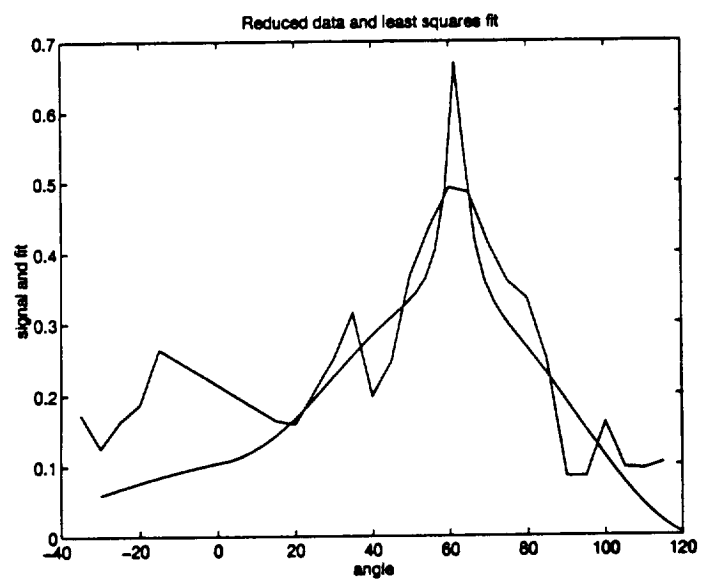


Figure J.8: Raw Signal and Fit - Composite Sample

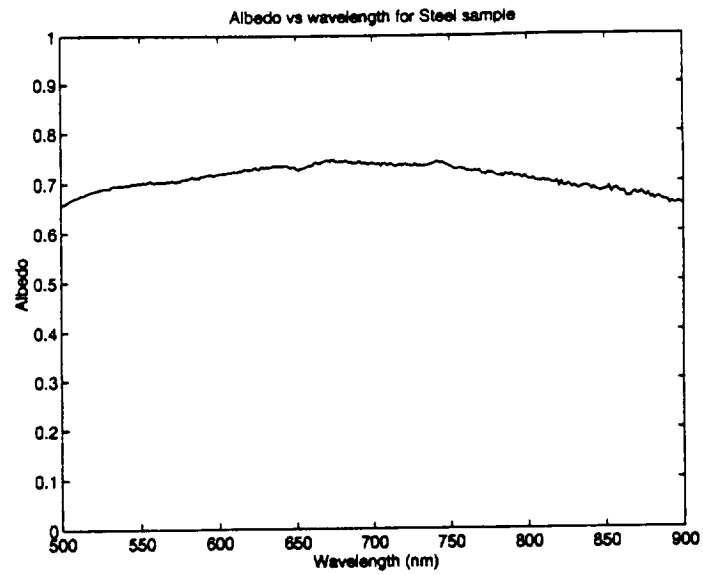


Figure J.9: Albedo - Steel Sample

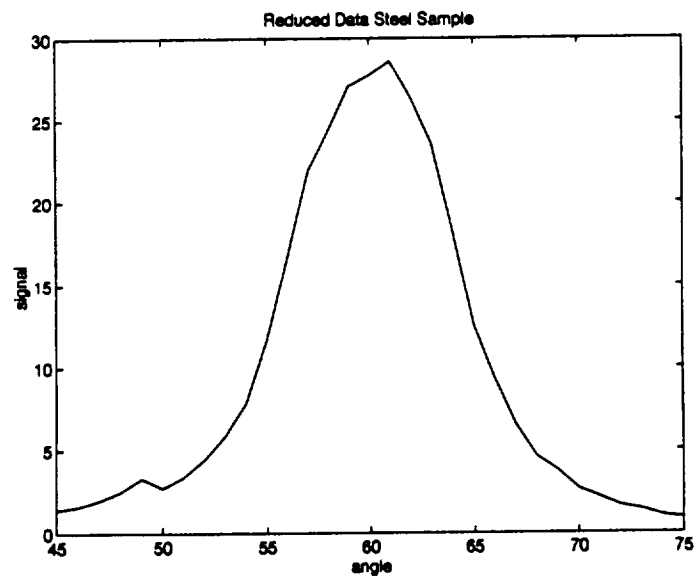


Figure J.10: Raw Signal - Steel Sample